



HAL
open science

Effect of dislocation density on competitive segregation of solute atoms to dislocations

W. Mottay, P. Maugis, M. Jouiad, F. Roch, C. Perrin-Pellegrino, K. Hoummada

► To cite this version:

W. Mottay, P. Maugis, M. Jouiad, F. Roch, C. Perrin-Pellegrino, et al.. Effect of dislocation density on competitive segregation of solute atoms to dislocations. *Materials Science and Engineering: A*, 2023, pp.145380. <10.1016/j.msea.2023.145380>. <hal-04146095>

HAL Id: hal-04146095

<https://u-picardie.hal.science/hal-04146095v1>

Submitted on 4 Apr 2024

HAL is a multi-disciplinary open access archive for the deposit and dissemination of scientific research documents, whether they are published or not. The documents may come from teaching and research institutions in France or abroad, or from public or private research centers.

L'archive ouverte pluridisciplinaire **HAL**, est destinée au dépôt et à la diffusion de documents scientifiques de niveau recherche, publiés ou non, émanant des établissements d'enseignement et de recherche français ou étrangers, des laboratoires publics ou privés.



HAL Authorization

Effect of dislocation density on competitive segregation of solute atoms to dislocations

W. Mottay^{1,2}, P. Maugis¹, M. Jouiad³, F. Roch², C. Perrin-Pellegrino¹, K. Hoummada^{1,*}

¹Aix Marseille Université, CNRS, IM2NP, 13397 Marseille, France

²Framatome, Développement (DTID) et Ingénierie Mécanique (DTIM), 92084 Paris la Défense Cedex, France

³Laboratory of Physics of Condensed Matter, University of Picardie Jules Verne, Scientific Pole, 33 rue Saint-Leu, 80039 Amiens Cedex 1, France

* Corresponding author, khalid.hoummada@im2np.fr

Abstract

We report on both experimental and modeling of carbon and nitrogen segregation to dislocations in C-Mn ferritic steels. A model based on McLean theory is established to describe the competitive segregation of carbon and nitrogen in the Cottrell atmospheres around dislocations, taking into account the effect of dislocation density. It is expected from the model that a high dislocation density strongly depletes interstitial atoms from the matrix, resulting in a low excess quantity of atoms on dislocations. Atom probe tomography analyses performed on two different C-Mn weld steels are in accordance with the model: carbon excess is tenfold higher in comparison to nitrogen excess in the deposited metal. However, after tensile test up to failure, this trend is no longer valid and nitrogen segregates preferentially than carbon. This suggests that plastic strain can modify the material properties by changing the nature and quantity of segregated atoms around dislocations.

Keywords

Segregation; dislocations; steel; welding; atom probe tomography

Highlights

- Modeling of carbon and nitrogen competitive segregation to dislocations.
- Low dislocation density favors carbon segregation in Cottrell atmospheres.
- Intermediate dislocation density favors nitrogen segregation.
- High dislocation density depletes the solid solution and the Cottrell atmospheres.
- Direct observation of nitrogen segregation on dislocations in a C-Mn steel.

Introduction

Carbon and nitrogen atoms are common alloying elements in iron, occupying the octahedral sites of both the body centered and face centered cubic structures. These interstitial atoms generate strong lattice distortion and hence considerably strengthen steels. It has been widely reported that these solutes tend to segregate on structural defects, such as interfaces and dislocations, in order to reduce the system free energy.

Regarding the interaction between solutes and dislocations, Cottrell and Bilby [1] proposed in 1948 that foreign atoms in solid solution can diffuse toward dislocations in order to relax the stress caused by the presence of defects, creating a so-called “Cottrell atmosphere” around the dislocation lines. These clouds of impurities decorating the dislocations play a major role in the mechanical [2,3] or electrical properties [4,5]. In bcc steels, segregation of solutes to dislocations was reported to have a deleterious effect on mechanical properties of the material, such as an increase of the brittle-ductile transition temperature and a loss of ductility [6–10].

The phenomenon of “strain-aging”, a modification of the mechanical properties due to the segregation of solute atoms to dislocations, has been extensively studied in the literature. In C-Mn ferritic steels, interstitial carbon and nitrogen are known to be responsible for the hardening observed after the steel has been plastically strained [11–13]. In most of the applications, the segregation of nitrogen to dislocations is not considered, as this element is precipitated thanks to the presence of strong nitride formers in the matrix, such as Ti, Nb, Al. However, some specific industrial applications cannot contain these elements in solid solution.

This concerns some weld steels for nuclear power plants. Nitride-forming elements cannot be included in the deposited metal. During the welding operation, they would oxidize at the contact of ambient oxygen before precipitating the interstitial nitrogen in the steel. As a result, there would still be interstitial nitrogen in the steel, as well as oxide inclusions, deleterious for the mechanical properties of the weld. Therefore, the weld metal contains both carbon and nitrogen in solid solution.

Even though nitrogen effect on strain-aging is well known [12,14], there are no systematic studies focused on the segregation of nitrogen to dislocations in steels. Moreover, the effect of a relatively high dislocation density, as found in weld metal, must be considered. This work intends to provide insights on carbon and nitrogen segregation to dislocations in C-Mn steel welds. First, the competitive segregation of carbon and nitrogen to dislocations is modeled based on McLean theory where the dislocation density is considered. Then, experimental results of carbon and nitrogen segregation to dislocations are presented.

Modeling

In order to comprehend the strain aging phenomena in welded steels containing both carbon and nitrogen in solid solution, their respective segregation to dislocations was modeled, based on McLean's theory of equilibrium segregation, applied to the segregation on dislocations [15,16]. The diffusion of interstitial atoms in ferritic steel is fast enough to neglect the segregation kinetics, considering the important operating time of a nuclear power plant. The McLean model was modified by Guttmann to describe the competitive segregation of carbon and nitrogen [17].

$$N_d^i = \frac{N_d N_b^i \exp\left(\frac{E_i}{kT}\right)}{N_b + N_b^N \exp\left(\frac{E_N}{kT}\right) + N_b^C \exp\left(\frac{E_C}{kT}\right)} \quad (1)$$

N_d^i and N_b^i are the number of interstitial atoms occupying the dislocation sites and the bulk sites respectively, in a unit volume. N_d and N_b represent respectively the total numbers of dislocation sites and bulk sites available. E_i is the segregation energy of element i to the defect (in eV), k is the Boltzmann constant and T is temperature.

Interstitial carbon and nitrogen occupy only the octahedral sites of the bcc crystal. As there are three octahedral sites per iron atom, the number of sites per unit volume is $N_b = \frac{3}{V_{Fe}}$, where V_{Fe} is iron atomic volume.

The segregation of carbon and nitrogen is site-competitive as both elements occupy the same type of sites, the octahedral ones, but one specific octahedral site can only be occupied by one atom, carbon or nitrogen.

The number of segregation sites per unit length on a single dislocation is expressed by parameter l . Based on the theoretical work of Veiga and al. [18] we considered a value of 150 sites per nanometer of dislocation. Finally, the number of segregation sites on all dislocations in a defined volume, N_d , expressed in nm^{-3} , depends on the dislocation density ρ (nm^{-2}), such as $N_d = \rho l$.

Taking into account the depletion of the solid solution, we can write the following material balance, where N_T^i is the total quantity of interstitial atoms per unit volume:

$$N_b^i = N_T^i - N_d^i \quad (2)$$

Da Rosa et al. [19] have developed the definition of the excess quantity on a dislocation, Γ^i in $\text{at} \cdot \text{nm}^{-1}$, of atoms i per unit length of dislocations, such as $\Gamma^i = \frac{N_d^i}{\rho}$.

As a consequence:

$$\Gamma^i = \frac{1}{\rho} * \frac{N_d(N_T^i - N_d^i) \exp\left(\frac{E_i}{kT}\right)}{N_b + (N_T^N - N_d^N) \exp\left(\frac{E_N}{kT}\right) + (N_T^C - N_d^C) \exp\left(\frac{E_C}{kT}\right)} \quad (3)$$

Using variable A_c defined as:

$$A_c = \frac{N_b + (N_T^N - N_d^N) \exp\left(\frac{E_N}{kT}\right)}{\exp\left(\frac{E_C}{kT}\right)} + N_d + N_T^C \quad (4)$$

We can write the excess of carbon and nitrogen on dislocations, taking into account the depletion of the solid solution:

$$\Gamma^C = \frac{1}{2\rho} * \left[A_c - \sqrt{A_c^2 - 4N_d N_T^C} \right] \quad (5)$$

Nitrogen excess Γ^N is symmetrical to Γ^C and can be calculated by switching the nitrogen and carbon related terms.

Thus, the equilibrium excess quantity of nitrogen and carbon on dislocations depends on their segregation energies, the concentration of carbon and nitrogen in solid solution and the dislocation density. It is worth noting that we did not consider any chemical interactions between the segregating solutes.

Modeling result

Effect of the segregation energies

Fig. 1 presents the calculated carbon excess quantity on dislocations as a function of carbon and nitrogen segregation energies.

The segregation energies used are in the range 0.2 – 0.5 eV, values commonly found in the literature [18,20]. The graph clearly shows that a slight change in the segregation energies used in the calculations drastically modifies the calculated excess quantity on dislocations. The dislocation density of 10^{14} m^{-2} is based on experimental values available in the literature [21,22]. The concentration of carbon is taken as 200 ppm.at (43ppm.wt), a value typical of low carbon steel. Nitrogen's concentration is taken as 400 ppm.at (100 ppm.wt) in accordance with studies on a similar material [7,23,24].

From Fig. 1, it is shown that a slight change in the segregation energies used in the model drastically modifies the calculated excess quantities. Indeed, considering a fixed segregation energy for nitrogen of 0.3 eV, carbon excess ranges from about 10 at.nm^{-1} for a carbon segregation energy of 0.25 eV, to more than 140 at.nm^{-1} for a segregation energy of 0.45 eV. This underlines the magnitude of a potential interaction between solutes, such as Mn-C, Mn-N or Cr-C, Cr-N interactions [25–27]. However, based on experimental excess values, the model allows for a precise

determination of segregation energies, taking into account the interactions between solutes.

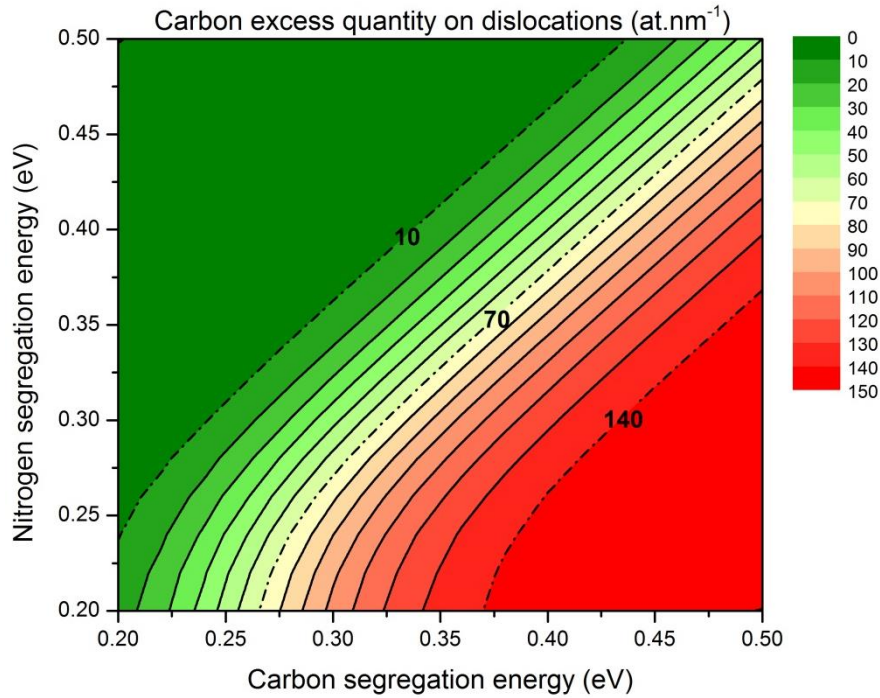


Figure 1: Calculated value of the carbon excess quantity on dislocations as a function of nitrogen and carbon segregation energies. Considered parameters are as follow: $T = 300\text{K}$; $\rho = 10^{14}\text{m}^{-2}$; $l = 150\text{at.nm}^{-1}$; $[C]_T = 200\text{ppm.at}$; $[N]_T = 400\text{ppm.at}$. It is shown that a slight change in the segregation energies, in the range of values commonly found in the literature, drastically modify the excess quantity calculated.

Effect of the dislocation density

Fig. 2 (a) and (c) present the calculated carbon and nitrogen excesses as a function of dislocation density, for two different values of free carbon and nitrogen concentrations in solution. The sum of both excesses is shown in blue. Fig. 2 (b) and (d) present the concentrations of carbon and nitrogen remaining in solid solution, as a function of the dislocation density. The concentrations used in Fig. 2 (a) and (b) are the same as the ones used in Fig. 1. The concentrations used in Fig. 2 (c) and (d) are lower, corresponding to the ones observed after post weld heat-treatment. Fig. 2 (b) and (d) exhibits the variations of carbon and nitrogen concentration in solid solution. All calculations were performed at $T = 300\text{K}$. The segregation energies used are 0.4 eV for carbon and 0.25 eV for nitrogen. Carbon segregation energy is in accordance with available data in the literature [18,20]. Nitrogen segregation energy is supposed to be slightly lower, as nitrogen segregation to grain boundaries has been reported to be lower than carbon segregation [28].

Fig. 2 (a) and (c) both show an important carbon excess for low dislocation densities, up to about 10^{14} m^{-2} , and a low one for nitrogen. It can be explained by the higher segregation energy of carbon, compared to nitrogen: even though carbon content in solid solution is lower than nitrogen content, carbon segregates preferentially than nitrogen to dislocations.

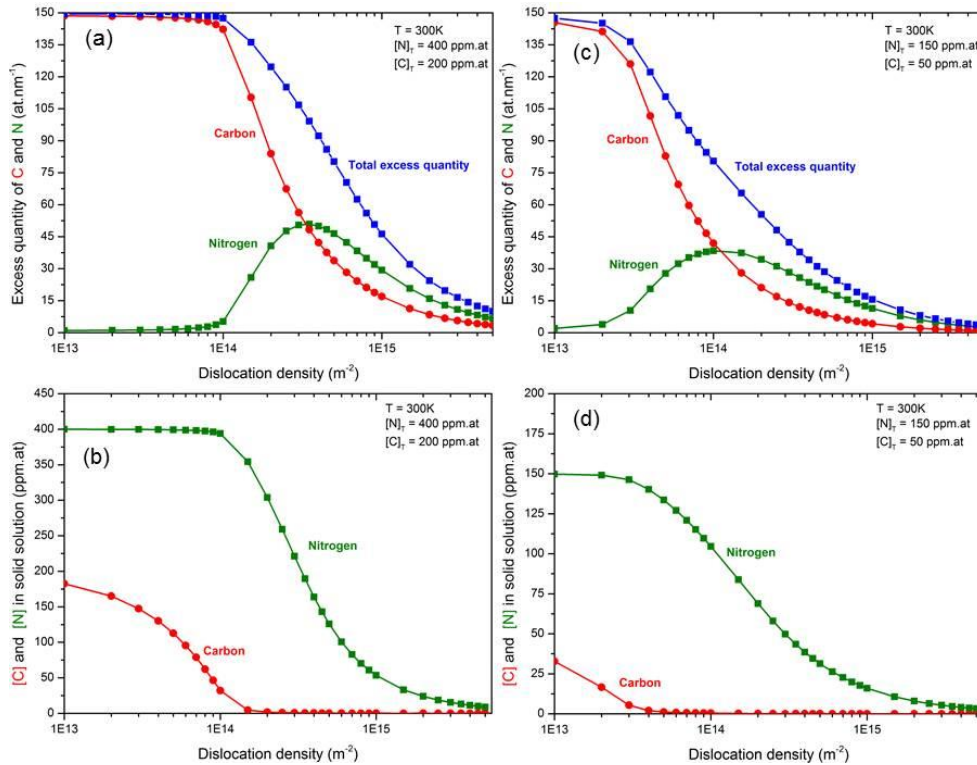


Figure 2: (a) Calculated carbon and nitrogen excess quantity (at.nm^{-1}) on dislocations as a function of dislocation density (m^{-2}). (b) Carbon and nitrogen remaining in solid solution as a function of dislocation density. For (a) and (b) the free concentration of carbon and nitrogen is 200 ppm.at and 400 ppm.at, respectively. (c) Calculated carbon and nitrogen excess quantity on dislocations as a function of dislocation density. (d) Carbon and nitrogen remaining in solid solution. For (c) and (d), the free concentration of carbon and nitrogen is 50 ppm.at and 150 ppm.at

An increasing dislocation density leads to an increased nitrogen excess at the expense of carbon. This relies on the fact that carbon solid solution has been depleted by the formation of dense Cottrell atmospheres. As a consequence, nitrogen excess increases as there is far more nitrogen than carbon in solution. For even higher dislocation densities, beyond 10^{15} m^{-2} , nitrogen and carbon excesses both reduce and tend to nil, because the solid solution is nearly fully depleted. This is interpreted as dislocations being essentially free from any interstitial atoms.

The main difference between Fig. 2 (a) and (c) relies on the lower concentration of free interstitials in (c). In this case, the same behavior is observed as in (a), but shifted to the lower dislocation densities. Indeed, as there are less interstitials atoms

in the matrix, a smaller number of segregation sites, i.e. dislocation density, is required to deplete the solid solution.

Finally, we can pay interest to the points where nitrogen excess crosses carbon excess. In these specific conditions, nitrogen and carbon excesses are equal. However, the model predicts that the remaining nitrogen concentration in solution is 300 times higher than carbon. We introduce the notion of “segregation power” defined as the ratio of the segregating elements concentration remaining in solution when their excesses are equal. In these conditions, carbon “segregation power” is 300 fold higher than nitrogen one at 300K. In short, to compensate their difference in segregation energy and obtain the same excess of carbon and nitrogen on dislocations, it is required to have 300 times more nitrogen remaining in solution than carbon.

The results exposed in Fig. 1 and 2 allow for a better understanding of the effect of nitrogen in the strain-aging of steels. Even in the case of ultra-low carbon steels, the segregation of carbon to dislocations is always observed. Straining the material (by welding, rolling or forming operations) leads to an increase of the dislocation density, reducing carbon excess on dislocations, thereby lowering the material’s sensibility to strain-aging. However, in the presence of nitrogen, straining the material leads to a reduction of carbon segregation but it allows for an increased segregation of nitrogen. Thus, the total excess on dislocations is less lowered because of the presence of nitrogen. In short, it is expected that a “reference” material exhibits mainly carbon’s segregation to dislocations and a strained material exhibits mainly nitrogen’s segregation to dislocations.

Materials and experimental techniques

Atom probe tomography (APT) analyses were performed on two C-Mn ferritic weld steels, carried out by manual metal arc welding. The time elapsed to cool down from 800 to 500°C after welding is estimated to 5 seconds, equivalent to a cooling rate of 60°C/s. The compositions of both steels are presented in Table 1. Steel 1 is the reference material, in the-as welded state. Steel 2 received a post weld heat-treatment at 600°C for 90 minutes. It was then strained at 300°C up to failure. Samples were taken from the root of the weld. It is worth mentioning that both steels do not have the same chemical composition. Unfortunately, Steel 2 contains 0.5% molybdenum. However, it is supposed that the presence of molybdenum will not modify the expected results, strong carbon segregation for Steel 1 and increased nitrogen segregation in Steel 2. The microstructure is composed of acicular ferrite and grain-boundary ferrite. Details of welded steels microstructures can be found elsewhere [29–31]. APT analyses were performed at 50K, 20% pulse fraction and 0.5% evaporation rate on a CAMECA LEAP 3000 XHR.

Table 1: Chemical compositions of the two steels studied. Compositions are given in % at (% wt).

	C	Mn	Si	N	Mo	Cr	V
Steel 1	0.3 (0.065)	1.39 (1.37)	0.54 (0.27)	0.056 (0.014)	∅	∅	∅
Steel 2	0.43 (0.092)	1.11 (1.09)	1.08 (0.54)	0.016 (0.004)	0.32 (0.54)	0.03 (0.03)	0.01 (0.01)

The N^+ and Si^{2+} mass-to-charge peaks are overlapped at 14 Da. The decomposition of the 14 Da peak was performed by studying the isotopic ratio of Si [32–34]. The number of counts in each peak at 14, 14.5 and 15 Da is measured. Neglecting the ^{15}N isotope, which abundance is inferior to 0.5%, we calculate the theoretical abundance of $^{28}Si^{2+}$ based on the measurements of $^{29}Si^{2+}$ and $^{30}Si^{2+}$ (peaks at 14.5 and 15 Da). If the measured counts of the 14 Da peak is superior to the maximum theoretical value calculated, the excess atoms in the 14 Da peak are attributed to $^{14}N^+$.

Experimental results

The experimental section aims at providing examples illustrating the model presented above. These examples are taken from industrial welds, but the focus of the manuscript is not on the physical metallurgy of welding.

Steel 1, reference material

Fig. 3 (a) shows a 3 million atoms volume in which only iron and carbon atoms are presented in grey and red, respectively. Fig. 3 (b) presents the 2% iso-concentration of carbon. It is clear that carbon has segregated along a line, crossing the specimen. This is interpreted as a Cottrell atmosphere around a dislocation, in accordance with [35]. Fig. 3 (c) presents the cumulative excesses of carbon, nitrogen and manganese as a function of the distance from the dislocation core. The core of the dislocation was defined as a 10% iso-concentration of carbon.

The excess quantity of solutes segregated on the dislocation was calculated using the method proposed by Da Rosa et al. [19]. A cylindrical region of interest around the dislocation is analyzed and compared to an identical volume far away from the dislocation. From Fig. 3 (c), it can be seen that three elements segregate along a dislocation: carbon, manganese and nitrogen. The extent of the Cottrell atmosphere is considered to be approximately 7.5 nm away from the dislocation center, corresponding to a distance where carbon excess seems to reach a plateau. This experimental value is in accordance with the theoretical work of Cocharadt and al. [36]. The excess values are 125 at.nm^{-1} for carbon, 20 at.nm^{-1} for manganese and 10

at.nm⁻¹ for nitrogen. As expected from Fig. 2, this reference material, Steel 1, exhibits important carbon segregation, low nitrogen one, with a dislocation density in the order of 10¹⁴ m⁻², as determined by TEM images using the cross lines conventional methods, and in accordance with the literature [21].

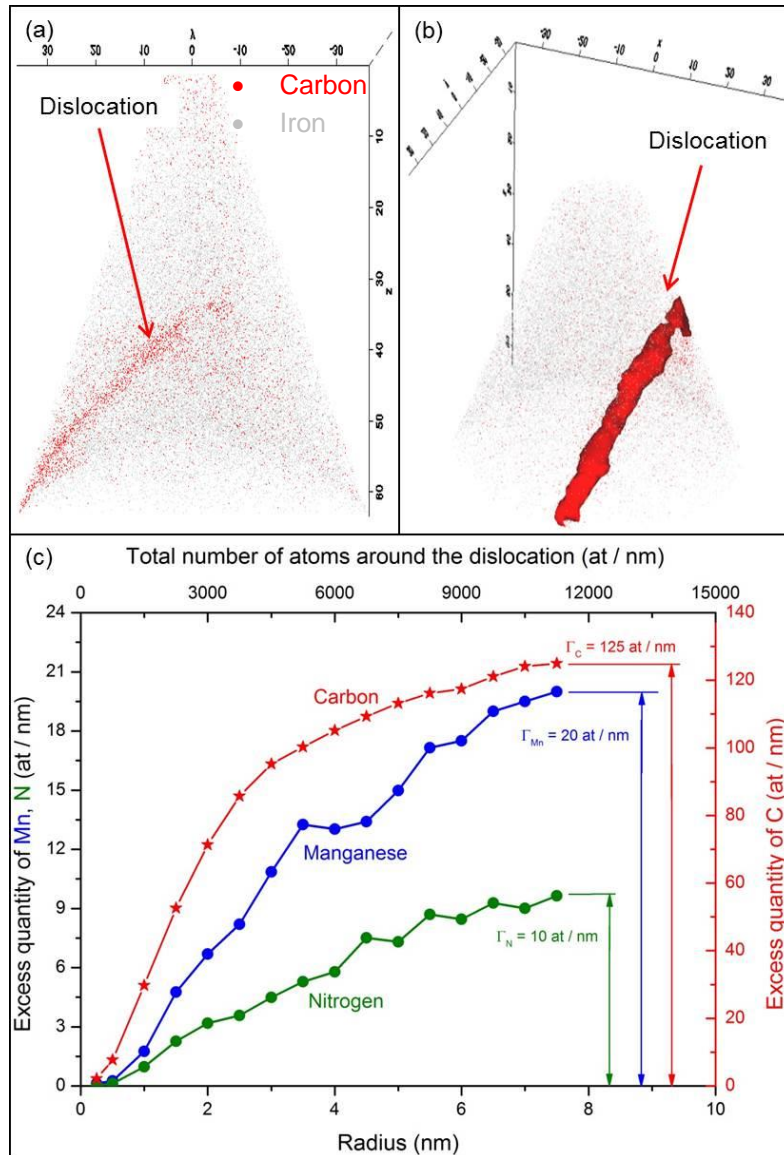


Figure 3: APT reconstructed volume from steel 1. (a) shows the repartition of carbon (red) and iron (grey). For clarity, other atoms are not presented. (b) presents a 2% iso-concentration of carbon. The probed volume contains a dislocation, evidenced by the iso-concentration of carbon segregated along a line crossing the volume. (c) Cumulative excess quantity of elements segregated along the dislocation, in at.nm⁻¹, as a function of the distance from the dislocation core.

Steel 2, strained material

APT analyses were also performed on steel 2, heat treated at 600°C for 90min and then tensile tested at 300°C up to failure. APT samples were collected 1 mm away

from the necking zone. Fig. 4 (a) shows a 1 million atom reconstructed volume in which only nitrogen, carbon and iron atoms are mapped, respectively in green, red and grey. The 0.8% iso-concentration shown in (b) is interpreted as a curved dislocation on which nitrogen is segregated, whereas (c) displays a 0.6% carbon iso-concentration.

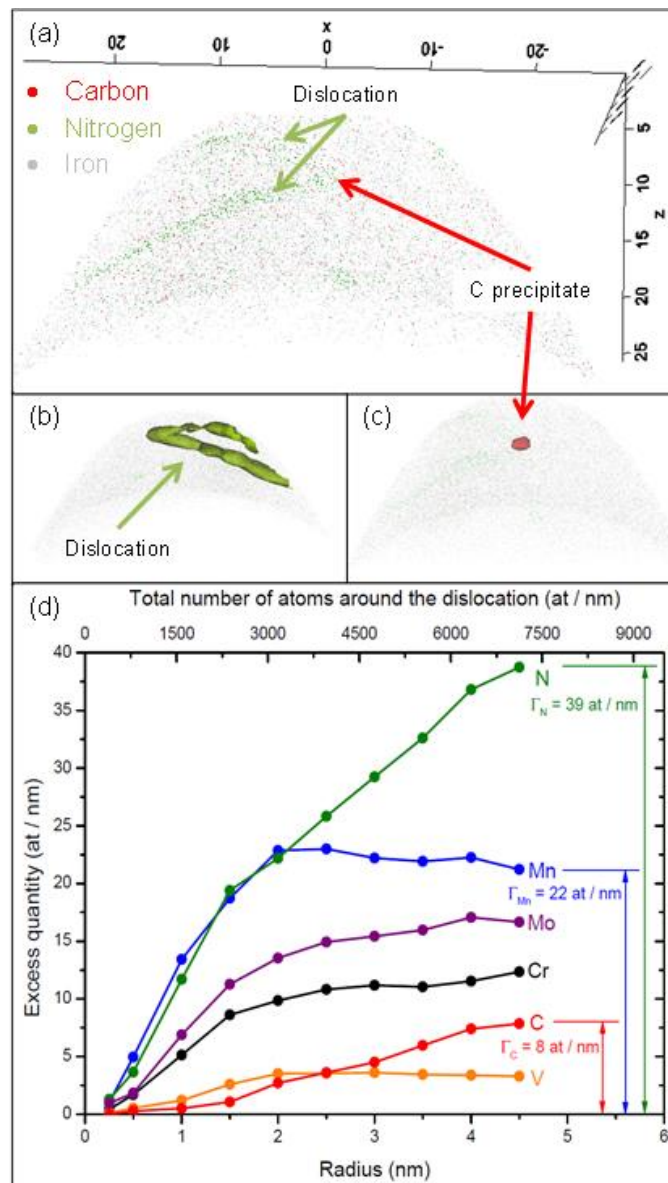


Figure 4: APT reconstructed volume from steel 2, after tensile test at 300°C up to failure. (a) the element repartition of carbon (red), nitrogen (green) and iron (grey) atoms. For clarity, other atoms are not represented. (b) 0.8% iso-concentration of nitrogen. The probed volume contains a curved dislocation pinned by a C precipitate. (c) a 0.6% iso-concentration of carbon. (d) Excess quantity of elements segregated along the dislocation, expressed in $\text{at}\cdot\text{nm}^{-1}$, as a function of the distance from the dislocation core.

The cumulative excess quantity of each element segregated along the bottom of the dislocation is presented in Fig. 4 (d). The top segment of the dislocation was not analyzed as it is too close to the APT sample tip surface. From this graph, the extent of the Cottrell atmosphere is evaluated to be only a 4.5 nm radius around the dislocation. Indeed, the small quantity of atoms collected by the APT and the presence of a second dislocation segment require reducing the analyzed volume around the dislocation. However, the excess quantity of substitutional elements seems to have already reached a plateau.

The excess quantities of carbon and nitrogen in steel 2 are very different from steel 1: the nitrogen excess quantity reaches 39 at.nm⁻¹ in the heat-treated sample, instead of 10 at.nm⁻¹ in steel 1. Meanwhile, the carbon excess quantity hardly reaches 8 at.nm⁻¹, a surprisingly low value compared to 125 at.nm⁻¹ in steel 1.

The results exposed in Fig. 3 and Fig. 4 are in accordance with the model developed in the first part of this paper. Indeed, the APT analyses performed in both steels 1 and 2 clearly show that the behavior of nitrogen and carbon regarding their segregation to dislocations is highly sensitive to the dislocation density. In the as-welded condition with a dislocation density in the order of 10¹⁴ m⁻², a high magnitude segregation of carbon is observed. However, in steel 2, which was strained at 300°C up to failure, carbon excess is rather low and nitrogen excess has increased. It could be argued that the different nominal composition of the steels may explain the different segregations observed. Statistics based on numerous APT analyses on the two samples show that they nearly have the same carbon content in solid solution. The average carbon concentration in steel 1 is about 400 at.ppm, this value is 250 at.ppm for steel 2. The presence of Mo may have increased nitrogen segregation energy. However, the total excess of interstitial atoms is rather low. An important increase of nitrogen segregation energy thanks to the presence of Mo should have increased the total excess of interstitial atoms. Fig. 2 (c) shows that for a dislocation density of 10¹⁴ m⁻², the total interstitial excess is about 75 at.nm⁻¹. In other words, half the available segregation sites are occupied by an interstitial atom. If nitrogen segregation energy was significantly increased by the presence of Mo on the dislocation, this would result in an increased total excess of interstitials. Thus, we conclude that nitrogen excess is increased because the dislocation density has increased and has depleted carbon from the matrix.

The effect of grain boundaries segregation and C or N clustering was neglected. Indeed, in the materials studied, the grain size is too important to significantly deplete C or N in solid solution [37]. We paid attention to the presence of C-N clusters or transition carbonitrides [38–40]. Their estimated density was sufficiently low to conclude that they have a negligible effect on C and N segregation.

Our experimental excess values are in good agreement with the ones calculated in our model, taking segregation energies of 0.4 eV for carbon and 0.25 eV for nitrogen. In Fig. 2 (a), we calculated an excess of 142 at.nm⁻¹ for carbon and 5 at.nm⁻¹ for

nitrogen, considering a dislocation density of 10^{14} m^{-2} , close to the experimental ones presented in Fig. 3. In Fig. 2 (c) we calculated an excess of 8 at.nm^{-1} for carbon and 20 at.nm^{-1} for nitrogen, with a dislocation density of 5.10^{14} m^{-2} , coherent with the values presented in Fig. 4.

Conclusion

We have shown that solute segregation to dislocations strongly depletes the solid solution, for dislocation densities superior or equal to 10^{14} m^{-2} , in the same way as reported by Danoix et al. where grain boundaries segregation can strongly deplete the matrix [37]. This dislocation density corresponds to the one observed in deformed steels, such as welds, rolled plates or deformed automotive parts. The depletion of the solid solution by the diffusion of interstitials to dislocations in these steels may modify the material properties. Moreover, a sufficiently low concentration of free interstitial atoms combined to a sufficiently high dislocation density prevents the formation of dense Cottrell atmosphere. This was observed experimentally by Samek et al. [38]. They show that the bake hardening values of low-alloy steels decrease when the pre-strain reaches important value, beyond 5%.

In this work, segregation of carbon and nitrogen to dislocations in a C-Mn weld steel was experimentally studied and modeled. As expected, there are experimental evidences that carbon segregates preferentially to dislocations than nitrogen. At the authors' best knowledge, this work is the first direct observation of nitrogen segregation to dislocations in steel.

The competitive segregation of both elements to dislocations was modeled, taking into account the initial concentrations in solution, segregation energies and the dislocation density. The model suggests that an important dislocation density may deplete carbon atoms from the matrix, thus reducing carbon excess at the expense of nitrogen. A sufficiently high dislocation density compared to the concentrations in solution leads to a low excess on dislocations, because of the depletion of interstitial atoms from the solid solution. This model could serve as a basis to adjust mechanical properties based on elements concentrations in the matrix or on excess on dislocations, in steels and in other metals.

Acknowledgements

This project was supported by the National Association of Research and Technology, France (ANRT Project n° 2020 / 0883).

Conflicts of interest

The authors have no conflicts of interest to declare

Data availability

All the necessary data is available in the main text. Any other relevant data are available upon request, with the exception of the full original POS files obtained from APT measurements, since these sets of data contain additional information unrelated to the subject of this study, which are the property of FRAMATOME.

References

- [1] A.H. Cottrell, B.A. Bilby, Dislocation Theory of Yielding and Strain Ageing of Iron, *Proc. Phys. Soc. Sect. A.* 62 (1949) 49–62. <https://doi.org/10.1088/0370-1298/62/1/308>.
- [2] G. Hachet, D. Caillard, L. Ventelon, E. Clouet, Mobility of screw dislocation in BCC tungsten at high temperature in presence of carbon, *Acta Mater.* 222 (2022) 117440. <https://doi.org/10.1016/j.actamat.2021.117440>.
- [3] P. Kontis, Z. Li, D.M. Collins, J. Cormier, D. Raabe, B. Gault, The effect of chromium and cobalt segregation at dislocations on nickel-based superalloys, *Scr. Mater.* 145 (2018) 76–80. <https://doi.org/10.1016/j.scriptamat.2017.10.005>.
- [4] V.V. Kveder, W. Schröter, M. Seibt, A. Sattler, Electrical Activity of Dislocations in Si Decorated by Ni, *Solid State Phenom.* 82–84 (2001) 361–366. <https://doi.org/10.4028/www.scientific.net/SSP.82-84.361>.
- [5] M. Seibt, V. Kveder, W. Schröter, O. Voß, Structural and electrical properties of metal impurities at dislocations in silicon, *Phys. Status Solidi A.* 202 (2005) 911–920. <https://doi.org/10.1002/pssa.200460515>.
- [6] D.V. Wilson, B. Russell, The contribution of precipitation to strain ageing in low carbon steels, *Acta Metall.* 8 (1960) 12.
- [7] D. Wagner, J.C. Moreno, C. Prioul, Dynamic strain aging sensitivity of heat affected zones in C–Mn steels, *J. Nucl. Mater.* 252 (1998) 257–265. [https://doi.org/10.1016/S0022-3115\(97\)00279-1](https://doi.org/10.1016/S0022-3115(97)00279-1).
- [8] D.V. Wilson, B. Russell, The contribution of atmosphere locking to the strain-ageing of low carbon steels, *Acta Metall.* 8 (1960) 36–45. [https://doi.org/10.1016/0001-6160\(60\)90138-3](https://doi.org/10.1016/0001-6160(60)90138-3).
- [9] L.E. Steele, K.E. Stahlkopf, eds., *Assuring structural integrity of steel reactor pressure vessels: proceedings of the 1st International Seminar on "Assuring Structural Integrity of Steel Reactor Pressure Vessels"*, Applied Science Publishers, London, 1980.
- [10] M. Grumbach, *Vieillissement des aciers*, *Tech. Ing.* (1993). <https://doi.org/10.51257/a-v1-m235>.
- [11] P. Elsen, H.P. Hougardy, On the mechanism of bake-hardening, *Steel Res.* 64 (1993) 431–436. <https://doi.org/10.1002/srin.199301049>.
- [12] D.R.G. Achar, M. Koçak, G.M. Evans, Effect of nitrogen on toughness and strain age embrittlement of ferritic steel weld metal, *Sci. Technol. Weld. Join.* 3 (1998) 233–243. <https://doi.org/10.1179/stw.1998.3.5.233>.
- [13] L.J. Baker, J.D. Parker, S.R. Daniel, Mechanism of bake hardening in ultralow carbon steel containing niobium and titanium additions, *Mater. Sci. Technol.* 18 (2002) 541–547. <https://doi.org/10.1179/026708302225001741>.
- [14] S.T. Mandziej, The effect of nitrogen and strain aging of C-Mn steel welds, *Scr. Metall. Mater.* 27 (1992) 793–798. [https://doi.org/10.1016/0956-716X\(92\)90394-T](https://doi.org/10.1016/0956-716X(92)90394-T).
- [15] I. Medouni, A. Portavoce, P. Maugis, P. Eyméoud, M. Yescas, K. Houmada, Role of dislocation elastic field on impurity segregation in Fe-based alloys, *Sci. Rep.* 11 (2021). <https://doi.org/10.1038/s41598-020-80140-4>.

- [16] J. Takahashi, K. Kawakami, J. Hamada, K. Kimura, Direct observation of niobium segregation to dislocations in steel, *Acta Mater.* 107 (2016) 415–422. <https://doi.org/10.1016/j.actamat.2016.01.070>.
- [17] M. Guttman, Thermochemical Interactions Versus Site Competition in Grain Boundary Segregation and Embrittlement in Multicomponent Systems, *J. Phys. IV.* 05 (1995) C7-85-C7-96. <https://doi.org/10.1051/jp4:1995707>.
- [18] R.G.A. Veiga, M. Perez, C.S. Becquart, C. Domain, Atomistic modeling of carbon Cottrell atmospheres in bcc iron, *J. Phys. Condens. Matter.* 25 (2013) 025401. <https://doi.org/10.1088/0953-8984/25/2/025401>.
- [19] G. Da Rosa, P. Maugis, J. Drillet, V. Hebert, K. Hoummada, Co-segregation of boron and carbon atoms at dislocations in steel, *J. Alloys Compd.* 724 (2017) 1143–1148. <https://doi.org/10.1016/j.jallcom.2017.07.096>.
- [20] E. Clouet, S. Garruchet, H. Nguyen, M. Perez, C.S. Becquart, Dislocation interaction with C in α -Fe: A comparison between atomic simulations and elasticity theory, *Acta Mater.* 56 (2008) 3450–3460. <https://doi.org/10.1016/j.actamat.2008.03.024>.
- [21] J.R. Yang, H.K.D.H. Bhadeshia, The dislocation density of acicular ferrite in steel welds, *Welds J.* (1990). <https://www.phase-trans.msm.cam.ac.uk/2002/dislocation.density.pdf> (accessed February 25, 2022).
- [22] S.H. He, B.B. He, K.Y. Zhu, M.X. Huang, Evolution of dislocation density in bainitic steel: Modeling and experiments, *Acta Mater.* 149 (2018) 46–56. <https://doi.org/10.1016/j.actamat.2018.02.023>.
- [23] D. Wagner, N. Roubier, C. Prioul, Measurement of sensitivity to dynamic strain aging in C–Mn steels by internal friction experiments, *Mater. Sci. Technol.* 22 (2006) 301–307. <https://doi.org/10.1179/174328406X86155>.
- [24] J. Belotteau, Comportement et rupture d'un acier au C-Mn en présence de vieillissement sous déformation, 2009.
- [25] V. Massardier, J. Merlin, E. Le Patezour, M. Soler, Mn–C interaction in Fe–C–Mn steels: Study by thermoelectric power and internal friction, *Metall. Mater. Trans. A.* 36 (2005) 1745–1755. <https://doi.org/10.1007/s11661-005-0039-x>.
- [26] V. Massardier-Jourdan, D. Colas, J. Merlin, Role of Manganese and Chromium on the Segregation Kinetics of Carbon and Nitrogen to the Dislocations in Ferritic Steels, *Mater. Sci. Forum.* 539–543 (2007) 4303–4308. <https://doi.org/10.4028/www.scientific.net/MSF.539-543.4303>.
- [27] H. Abe, T. Suzuki, S. Okada, Decomposition of Mn–C Dipoles during Quench–Ageing in Low-Carbon Aluminium-Killed Steels, *Trans. Jpn. Inst. Met.* 25 (1984) 215–225. <https://doi.org/10.2320/matertrans1960.25.215>.
- [28] J. Takahashi, K. Kawakami, K. Ushioda, S. Takaki, N. Nakata, T. Tsuchiyama, Quantitative analysis of grain boundaries in carbon- and nitrogen-added ferritic steels by atom probe tomography, *Scr. Mater.* 66 (2012) 207–210. <https://doi.org/10.1016/j.scriptamat.2011.10.026>.
- [29] D.J. Abson, Acicular ferrite and bainite in C–Mn and low-alloy steel arc weld metals, *Sci. Technol. Weld. Join.* 23 (2018) 635–648. <https://doi.org/10.1080/13621718.2018.1461992>.
- [30] G.M. Evans, The Effect of Carbon on the Microstructure and Properties of C–Mn All-Weld Metal Deposits, (n.d.).
- [31] A.G. Olabi, M.S.J. Hashmi, The microstructure and mechanical properties of low carbon steel welded components after the application of PWHTs, *J. Mater. Process. Technol.* 56 (1996) 88–97. [https://doi.org/10.1016/0924-0136\(95\)01824-7](https://doi.org/10.1016/0924-0136(95)01824-7).
- [32] W. Sha, L. Chang, G.D.W. Smith, Liu Cheng, E.J. Mittemeijer, Some aspects of atom-probe analysis of Fe–C and Fe–N systems, *Surf. Sci.* 266 (1992) 416–423. [https://doi.org/10.1016/0039-6028\(92\)91055-G](https://doi.org/10.1016/0039-6028(92)91055-G).
- [33] A.J. London, Quantifying Uncertainty from Mass-Peak Overlaps in Atom Probe Microscopy, *Microsc. Microanal.* 25 (2019) 378–388. <https://doi.org/10.1017/S1431927618016276>.

- [34] F. Meisenkothen, D.V. Samarov, I. Kalish, E.B. Steel, Exploring the accuracy of isotopic analyses in atom probe mass spectrometry, *Ultramicroscopy*. 216 (2020) 113018. <https://doi.org/10.1016/j.ultramic.2020.113018>.
- [35] M.K. Miller, Atom probe tomography characterization of solute segregation to dislocations, *Microsc. Res. Tech.* 69 (2006) 359–365. <https://doi.org/10.1002/jemt.20291>.
- [36] A.W. Cochardt, G. Schoek, Interaction between dislocations and interstitial atoms in body-centered cubic metals, *Acta Metall.* 3 (1955) 5.
- [37] F. Danoix, K. Hoummada, P. Maugis, N. Rolland, C. Debreux, D. Blavette, Grain size effect on interfacial segregation in nanomaterials, *J. Phys. Chem. Solids*. 164 (2022) 110620. <https://doi.org/10.1016/j.jpcs.2022.110620>.
- [38] L. Samek, J. Dykas, E.D. Moor, A. Grajcar, Strain-Ageing of Low-Alloyed Multiphase High-Strength Steels, *Metals*. 10 (2020) 439. <https://doi.org/10.3390/met10040439>.